Anal. Chem. **2007,** *79,* 9030−9038

Typing of Multiple Single-Nucleotide Polymorphisms by a Microsphere-Based Rolling Circle Amplification Assay

Jishan Li and Wenwan Zhong*

Department of Chemistry, University of California, Riverside, California 92521

The combination of suspension array with rolling circle amplification can lead to a sensitive and specific assay for single-nucleotide polymorphisms (SNPs) detection, as demonstrated in this study. A circular template generated by ligation upon the recognition of a point mutation on DNA targets was amplified isothermally by the Phi29 polymerase on microspheres. The elongation products were labeled with fluorochrome-tagged probes and detected in a flow cytometer, indicating the mutation occurrence. As low as 10 amol of mutated strands was detected by this assay, and positive mutation detection was achieved with a wild-type to mutant ratio of 10 000:1, which could be attributed to the high amplification efficiency of Phi29, the high binding capacity of the microspheres, and the remarkable precision of DNA ligase in distinguishing mismatched bases at the ligation site. A novel design of using two differently labeled detection probes on the same microsphere to target both the wild-type and mutant samples allowed parallel determination of the heterozygosity for two SNPs (K-ras G12C and TP53 R273H) in PCR amplicons prepared from human genomic DNA extracts. This ability lays the groundwork for further enhancing the assay throughput by using multiple fluorophores and microspheres with distinct properties.

Single-nucleotide polymorphisms (SNPs) are the most common variations in human genomes.[1] Studies have found close associations between SNP and tumor development or progression, and SNPs detection has been believed to be a promising tool for early diagnosis and risk assessment of malignancy.[1−3] Moreover, SNP occurring in genes coding for enzymes critical for drug metabolism can induce various drug resistance and side effects in different individuals.[4] Comprehensive SNPs genotyping can achieve valuable information to guide the development of personal drugs and therapies.[5,6] SNPs may also be responsible for other phenotypic differences among individuals.[1] Because of the great importance of SNPs in disease diagnosis and cure, enormous attention has been paid to develop effective assays for SNPs screening after the completion of the Human Genome Project.[1,3]

Recent advents in technologies offer a wide variety of choices for SNP detection. Electrophoresis-based methods, such as sequencing, gradient gel electrophoresis,[7,8] single-stranded conformation polymorphism,[9−11] and heteroduplex analysis,[12] are reliable and straightforward. New developments further simplify the separation process with the introduction of polyamide drag-tags or a DNA binding protein specific for sequence mismatch,[13−15] and employment of microfluidic chips as the separation platforms makes it possible to perform high-throughput and fast screening for SNPs.[16,17] Approaches involving mass spectrometry (MS) aim to increase the accuracy in DNA variation detection by measuring the intrinsic property (molecular mass) of a nucleic acid.[18−20] Nevertheless, sensitivity is always a big issue in SNP typing. Polymerase chain reaction (PCR) is usually the unavoidable prerequisite to obtain a detectable amount of samples from genomic DNA. Microarray technologies coupled to enzymatic reactions such as PCR and ligation have been successfully applied

* Corresponding author. E-mail: wenwan.zhong@ucr.edu. Phone: 951-827-4925. Fax: 951-827-4713.

(1) Engle, L. J.; Simpson, C. L.; Landers, J. E. *Oncogene* **2006**, *25*, 1594−1601.
(2) Carlton, V. E. H.; Ireland, J. S.; Useche, F.; Faham, M. *Hum. Genomics* **2006**, *2*, 391−402.
(3) McCarthy, J. J.; Hilfiker, R. *Nat. Biotechnol.* **2000**, *18*, 505−508.
(4) Murray, M. *J. Pharm. Pharmacol.* **2006**, *58*, 871−885.
(5) Shastry, B. S. *BioMEMS Biomed. Nanotechnol.* **2006**, *2*, 447−458.
(6) Kroczak, T. J.; Baran, J.; Pryjma, J.; Siedlar, M.; Reshedi, I.; Hernandez, E.; Alberti, E.; Maddika, S.; Los, M. *Expert Opin. Ther. Targets* **2006**, *10*, 289−302.
(7) Bjorheim, J.; Ekstrom, P. O. *Electrophoresis* **2005**, *26*, 2520−2530.
(8) Li, Q.; Deka, C.; Glassner, B. J.; Arnold, K.; Li-Sucholeiki, X.-C.; Tomita-Mitchell, A.; Thilly, W. G.; Karger, B. L. *J. Sep. Sci.* **2005**, *28*, 1375−1389.
(9) Kuhn, D. N.; Borrone, J.; Meerow, A. W.; Motamayor, J. C.; Brown, J. S.; Schnell, R. J. *Electrophoresis* **2005**, *26*, 112−125.
(10) Doi, K.; Doi, H.; Noiri, E.; Nakao, A.; Fujita, T.; Tokunaga, K. *Electrophoresis* **2004**, *25*, 833−838.
(11) Tahira, T.; Okazaki, Y.; Miura, K.; Yoshinaga, A.; Masumoto, K.; Higasa, K.; Kukita, Y.; Hayashi, K. *Electrophoresis* **2006**, *27*, 3869−3878.
(12) Esteban-Cardenosa, E.; Duran, M.; Infante, M.; Velasco, E.; Miner, C. *Clin. Chem.* **2004**, *50*, 313−320.
(13) Vreeland, W. N.; Meagher, R. J.; Barron, A. E. *Anal. Chem.* **2002**, *74*, 4328−4333.
(14) Meagher, R. J.; Coyne, J. A.; Hestekin, C. N.; Chiesl, T. N.; Haynes, R. D.; Won, J.-I.; Barron, A. E. *Anal. Chem.* **2007**, *79*, 1848−1854.
(15) Drabovich, A. P.; Krylov, S. N. *Anal. Chem.* **2006**, *78*, 2035−2038.
(16) Li, Z.-p.; Tsunoda, H.; Okano, K.; Nagai, K.; Kambara, H. *Anal. Chem.* **2003**, *75*, 3345−3351.
(17) Erickson, D.; Liu, X.; Venditti, R.; Li, D.; Krull, U. J. *Anal. Chem.* **2005**, *77*, 4000−4007.
(18) Oberacher, H.; Niederstaetter, H.; Casetta, B.; Parson, W. *Anal. Chem.* **2005**, *77*, 4999−5008.
(19) Mengel-Jorgensen, J.; Sanchez, J. J.; Borsting, C.; Kirpekar, F.; Morling, N. *Anal. Chem.* **2005**, *77*, 5229−5235.
(20) Jiang, Y.; Hall, T. A.; Hofstadler, S. A.; Naviaux, R. K. *Clin. Chem.* **2007**, *53*, 195−203.

10.1021/ac701702t CCC: $37.00
Published on Web 11/01/2007

to detect low-abundant mutations in genomic DNA samples.[21,22] However, PCR could introduce errors into SNP detection during the exponential amplification process. To improve detection sensitivity and eventually eliminate the need for PCR, highly responsive detection tags other than fluorescent molecules have been used, such as quantum dots and gold or silver nanoparticles.[23−26]

Alternatively, replication reactions can be employed only to amplify signals after SNP recognition without affecting the quality of the templates. The GoldenGate assay utilizes PCR to amplify fragments generated by allele-specific extension and oligonucleotide ligation.[1,27] A remarkable chemical-based atom transfer radical polymerization developed by Lou et al. allows instrument-free detection of SNP.[28] Rolling circle amplification (RCA) is another simple replication method that can replace PCR. In RCA, a circular template is amplified isothermally by a DNA polymerase φ29 with excellent strand displacement properties. The long single-stranded DNA product contains thousands of sequence repeats that can serve as the detection sites.[29−32] The circular template can be synthesized from a padlock probe, the 5′ and 3′ termini of which can hybridize precisely onto the target and then be joined by a DNA ligase.[29,30] The stringent requirement of ligation on strand matching and the high amplification efficiency of RCA are exactly what an SNP typing assay needs to obtain high sensitivity and specificity. In addition, the isothermal reaction condition simplifies the adaptation of RCA to routine clinical usages.[29,30] Furthermore, the RCA signal can be confined locally if the amplification primer is immobilized onto a solid support, and the amplification rate on the template sequences is independent of the template sequences, making the design of multiplexed assay simpler.[29,30] One attomole of the synthetic DNA target was detected by RCA on a glass slide in a fluorescence microscope equipped with an intensified CCD camera.[33] Combined with an invasive cleavage assay, RCA allowed parallel SNP genotyping from unamplified human genomic DNA samples on small DNA arrays.[34]

Each method mentioned above has its own advantages and disadvantages with respect to simplicity, sensitivity, ease of multiplexing, throughput, and cost. Continuous improvements in SNP screening are still in demand. Here, we report a highly sensitive and specific assay for SNPs detection using a suspension array format. In comparison to the planar array on the flat surface, the suspension array using microspheres as the solid support offers several advantages, such as fast reaction kinetics in liquid phase, high binding capacity on the micrometer-sized beads which have large surface area-to-volume ratios, and feasibility of mixing different array elements as required for individual tests.[35−38] The microsphere-based assay presented here took advantage of the suspension array and amplified the SNP recognition events on the surface of microspheres by RCA before detection in a flow cytometer. Two padlock probes with the same primer amplification sites were designed to bind to detection probes labeled with distinct fluorescent dyes and target the wild-type and mutant sequences, respectively, allowing the assay to probe for sample heterozygosity with only one type of bead. Higher assay throughput can be achieved by employing microspheres with various sizes, as demonstrated by the detection of mutations at two loci in the K-ras and TP53 genes in our study.

EXPERIMENTAL SECTION

Oligonucleotides and Chemicals. All oligonucleotides were purchased from Integrated DNA Technologies (Coralville, IA) and were used as received. Table 1 lists the strands used for ligation, RCA, and detection. Point mutations of K-ras G12C (GGT → TGT) and TP53 R273H (CGT → CAT) were targeted in our study, and the cDNA regions about 20 nt upstream and downstream of the SNP sites were used in our design. The forward cDNA sequences comprised of the 3′ and 5′ arms of the padlock probes (Kras-G12C-N/M and TP53-R273H-N/M) and oligonucleotides with sequences in the corresponding regions on the reverse strands were used as the arbitrary targets (Target-Kras-N/M and Target-TP53-N/M). The 5′ ends of the padlock probes were phosphorylated for ligation, and those of the capture probes, CP1 and CP2, were labeled with amine groups for microsphere conjugation. The detection probes, DP1 and DP2, were tagged with FAM (6-carboxyfluorescein) and Cy3, respectively.

E. coli DNA ligase was from Takara Bio (Shiga, Japan). RepliPHI Phi29 DNA polymerase (100 U/μL) and the mixture of deoxyribonucleotides (dNTPs) were purchased from Epicentre (Madison, WI). Chemicals for oligonucleotides conjugation, 1-ethyl-3-(3-(dimethylamino)propyl)carbodiimide hydrochloride (EDC) and *N*-hydroxysulfosuccinimide (sulfo-NHS), were from Pierce Biotechnology (Rockford, IL). Magnesium chloride ($MgCl_2$), albumin from bovine serum (BSA), and β-nicotinamide adenine dinucleotide hydrate (NAD^+) were obtained from Sigma-Aldrich (St. Louis, MO). Other chemicals were all from Fisher Scientific (Fairlawn, NJ). Buffers were prepared in deionized water from a Milli-Q water purification system (Millipore, Billerica, MA). SPHERO Carboxyl polystyrene particles (Lake Forest, IL) of two different sizes, 5.28 and 3.17 μm, were employed for the four-plexed detection.

(21) Hashimoto, M.; Hupert, M. L.; Murphy, M. C.; Soper, S. A.; Cheng, Y.-W.; Barany, F. *Anal. Chem.* **2005**, *77*, 3243−3255.
(22) Favis, R.; Huang, J.; Gerry, N. P.; Culliford, A.; Paty, P.; Soussi, T.; Barany, F. *Hum. Mutat.* **2004**, *24*, 63−75.
(23) Gerion, D.; Chen, F.; Kannan, B.; Fu, A.; Parak, W. J.; Chen, D. J.; Majumdar, A.; Alivisatos, A. P. *Anal. Chem.* **2003**, *75*, 4766−4772.
(24) Li, J.; Chu, X.; Liu, Y.; Jiang, J.-H.; He, Z.; Zhang, Z.; Shen, G.; Yu, R. *Nucleic Acids Res.* **2005**, *33*, e168.
(25) Li, Y.; Wark, A. W.; Lee, H. J.; Corn, R. M. *Anal. Chem.* **2006**, *78*, 3158−3164.
(26) Liu, C.-H.; Li, Z.-P.; Du, B.-A.; Duan, X.-R.; Wang, Y.-C. *Anal. Chem.* **2006**, *78*, 3738−3744.
(27) Gunderson, K. L.; Steemers, F. J.; Lee, G.; Mendoza, L. G.; Chee, M. S. *Nat. Genet.* **2005**, *37*, 549−554.
(28) Lou, X.; Lewis, M. S.; Gorman, C. B.; He, L. *Anal. Chem.* **2005**, *77*, 4698−4705.
(29) Nilsson, M.; Dahl, F.; Larsson, C.; Gullberg, M.; Stenberg, J. *Trends Biotechnol.* **2006**, *24*, 83−88.
(30) Zhang, D.; Wu, J.; Ye, F.; Feng, T.; Lee, I.; Yin, B. *Clin. Chim. Acta* **2006**, *363*, 61−70.
(31) Baner, J.; Nilsson, M.; Mendel-Hartvig, M.; Landegren, U. *Nucleic Acids Res.* **1998**, *26*, 5073−5078.
(32) Blab, G. A.; Schmidt, T.; Nilsson, M. *Anal. Chem.* **2004**, *76*, 495−498.
(33) Nie, B.; Shortreed, M. R.; Smith, L. M. *Anal. Chem.* **2005**, *77*, 6594−6600.
(34) Chen, Y.; Shortreed, M. R.; Olivier, M.; Smith, L. M. *Anal. Chem.* **2005**, *77*, 2400−2405.
(35) Nolan, J. P.; Sklar, L. A. *Trends Biotechnol.* **2002**, *20*, 9−12.
(36) Edwards, B. S.; Oprea, T.; Prossnitz, E. R.; Sklar, L. A. *Curr. Opin. Chem. Biol.* **2004**, *8*, 392−398.
(37) Kellar, K. L.; Iannone, M. A. *Exp. Hematol.* **2002**, *30*, 1227−1237.
(38) McBride, M. T.; Masquelier, D.; Hindson, B. J.; Makarewicz, A. J.; Brown, S.; Burris, K.; Metz, T.; Langlois, R. G.; Tsang, K. W.; Bryan, R.; Anderson, D. A.; Venkateswaran, K. S.; Milanovich, F. P.; Colston, B. W., Jr. *Anal. Chem.* **2003**, *75*, 5293−5299.

Table 1. Oligonucleotides and Their Notations Used in the Present Study[a]

Kras-G12C-M	5′-phosphate-GTGGCGTAGGCAAGATAGAATGAAGATAGCGCATCGTAGGACTTATTTCGTAGGACTTAGGGTAGTTGGAGCT**T**-3′
Kras-G12C-N	5′-phosphate-GTGGCGTAGGCAAGATAGAATGAAGATAGCGCATGTAGAACTCACCTGTTTCAAAGGGTAGTTGGAGCT**G**-3′
TP53-R273H-M	5′-phosphate-TGTTTGTGCCTGTCCATGTTTAGTTGGTCACACGTTCGTAGGACTTAAAACAGCTTTGAGGTGC**A**-3′
TP53-R273H-N	5′-phosphate-TGTTTGTGCCTGTCCATGTTTAGTTGGTCACACGTGTAGAACTCACCTGTTTCTTTTTACAGCTTTGAGGTGC**G**-3′
Target-Kras-M	5′-ACTCTTGCCTACGCCAC**A**AGCTCCAACTACCACAAGTTT-3′
Target-Kras-N	5′-ACTCTTGCCTACGCCAC**C**AGCTCCAACTACCACAAGTTT-3′
Target-TP53-M	5′-GGACAGGCACAAACA**T**GCACCTCAAAGCTGTTCCGT-3′
Target-TP53-N	5′-GGACAGGCACAAACA**C**GCACCTCAAAGCTGTTCCGT-3′
CP1	5′-NH_2-C12-AAAAAAAAAAAAAAAAATGCGCTATCTTCA-3′
CP2	5′-NH_2-C12-AAAAAAAAAAAAAAAAACGTGTGACCAACTA-3′
DP1	5′-FAM-TCGTAGGACTTA-3′
DP2	5′-Cy3-AAAGTAGAACTCACCTGTTTC-3′

[a] The loci in interest are shown in bold.

Conjugation of Capture Probes on Microspheres. Coupling the amplification primers to the surface of microspheres was performed as follows. First, 6.3 nmol of the CP1 or CP2 was added to 4 mL of the 0.1 M phosphate buffer (pH 7.3) containing around 10^8 microspheres. Mixed with 26 mg of sulfo-NHS and 160 mg of EDC, the reaction mixture was stirred at room temperature for 4 h. Then the microspheres were centrifuged down at 5900*g* for 1 min. Following removal of the supernatant, the microspheres were washed twice with a solution of 0.1 M KCl, 4 mM $MgCl_2$, and 0.05% Tween 20 in 30 mM Tris−HCl (pH 7.8). The conjugated beads were then resuspended in 1 mL of the 0.1 M KCl−4 mM $MgCl_2$−30 mM Tris-HCl (pH 7.8) solution and stored in a refrigerator (4 °C).

To estimate the coupling efficiency and calculate the approximate number of capture probes (CPs) on each microsphere, a complementary probe labeled with FAM (5′-FAM-TAGAATGAAGATAGCGCATCG-3′, one FAM molecule per oligonucleotide) was used to incubate with the CP1-coupled beads in 100 μL of phosphate-buffered saline (PBS, with 0.3 M NaCl) for 4 h at 37 °C, and the resulted fluorescence was measured by a BD FACScan flow cytometer (Becton Dickinson, San Diego, CA). A calibration curve of fluorescence intensity versus molecules of equivalent soluble fluorochrome (MESF) was constructed with the same instrument settings using the Quantum FITC MESF kit (Bangs Laboratories, Fishers, IN), which was comprised of five populations of microspheres with known numbers of FITC molecules per bead. With the use of this curve, the number of capture probes immobilized on each microsphere was estimated to be about 3.46×10^5 per bead (or $3.95 \times 10^{11}/cm^2$) and was similar for both the 5.28 and 3.17 μm beads.

Point Mutation Detection. In a typical experiment, the oligonucleotide target in interest was hybridized to the padlock probe in 40 μL of ligation buffer (30 mM Tris−HCl, pH 7.8, 4 mM $MgCl_2$, 0.1 M KCl, 0.1 mM NAD^+) during a 60 min incubation at 45 °C. If the PCR amplicons were used, the reaction mixture was denatured at 98 °C for about 4 min and then immersed in ice−water rapidly before the incubation. Then, 3.6 U of *E.coli* DNA ligase, 1 μL of 2% BSA, and ~10^5 of the capture probe-coated beads were added to the mixture. After another incubation at 37 °C for 60 min, the microspheres were washed once using 200 μL of solution of 50 mM Tris−HCl, 50 mM KCl, and 10 mM $MgCl_2$. Polymerization was carried out at 37 °C for 30 min in 40 μL of Phi29 reaction buffer (40 mM Tris−HCl, pH7.5, 50 mM KCl, 10 mM $MgCl_2$, 5 mM $(NH_4)_2SO_4$, 4 mM DTT) with 1 U/μL Phi29 polymerase and 625 μM dNTP. The microspheres were washed again with 10 mM phosphate buffer (pH7.4), and 1 μM of the detection probe in 50 μL of PBS was added to the beads for another round of 30 min incubation at 37 °C. Finally, the beads were resuspended in 500 μL of PBS and analyzed in a flow cytometer. A MACSmix tube rotator (Miltenyi Biotec Inc., Auburn, CA) was used to shake the reaction tubes inside the incubation chamber to prevent bead aggregation.

Flow Cytometric Analysis. The FACScan system used in this study was equipped with a 488 nm air-cooled argon ion laser. In the flow cytometer, the microspheres were gated on forward light scatter and side (90°) light scatter, and the FAM and Cy3 signals were measured at the Fl1 (515−545 nm) and Fl2 (564−606 nm) channels, respectively, with compensation settings of Fl1−%Fl2 at 10.8 and Fl2−%Fl1 at 92.6. Median fluorescence intensity of 1000 gated beads and dot plots were obtained by the CellQuest software (Beckton Dickson).

PCR Amplification of Genomic DNA. Human genomic DNAs extracted from the colon cancer cell line HT29 and the lung cancer cell line NCI-H358 were purchased from ATCC (American Type Culture Collection). The primers used were as follows: forward = 5′AACCTTATGTGTGACATGTTCTAATATAGTCAC 3′ and reverse = 5′AAAATGGTCAGAGAAACCTTTATCTGTATC3′, for generation of an 254 bp amplicon from the K-ras gene;[25] forward = 5′GGACAGGTAGGACCTGATTTCCTTAC 3′ and reverse = 5′CGCTTCTTGTCCTGCTTGCTTAC 3′, for generation of a 219 bp PCR product from the TP53 gene.[23] PCR amplification was performed with the Phusion High-Fidelity PCR kit (New England BioLabs, Ipswich, MA). Briefly, 50 μL of the Phusion High Fidelity buffer containing 200 μM dNTPs and 0.5 μM forward and reverse primers was mixed with 50 ng of genomic DNA and 1 U of Phusion DNA polymerase. Amplification was achieved by thermal cycling for 30 cycles at 95 °C for 30 s, 60 °C for 30 s, and 72 °C for 1 min with a final extension at 72 °C for 10 min. PCR products were purified by phenol extraction, and dNTPs were removed by the CentriSpin 20 columns from Princeton Separations (Adelphia, NJ) before DNA sequencing and UV absorption measurement for concentration estimation.

RESULTS AND DISCUSSION

Rolling Circle Amplification on Microspheres. The schematic assay design is presented in Figure 1. DNA ligases are in charge of the last step of DNA repair and replication in host cells; thus, they join only the perfectly complementary DNA duplexes without resealing strand breaks with mismatched bases. This high fidelity of DNA ligases can be employed to discriminate single-

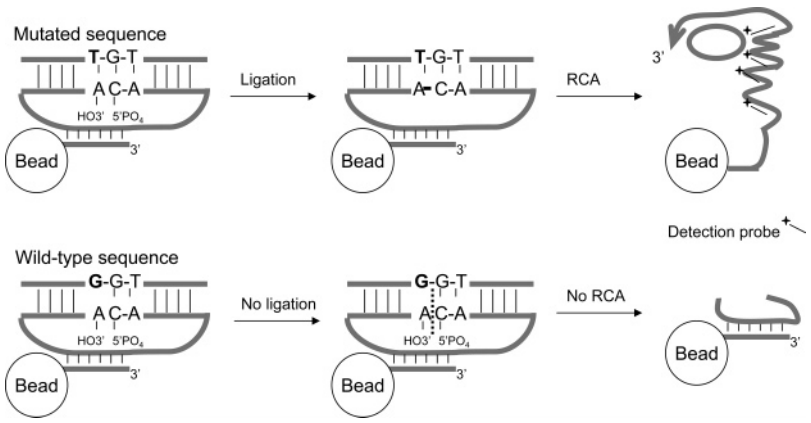

Figure 1. Schematic drawing of the microsphere-based RCA assay for SNP detection. The bases shown in bold are the mutation points.

nucleotide mutation.[22,23,39] Only when the padlock probe perfectly anneals to the target can the ligase link the 5′ and 3′ termini of the padlock probe together to form a circular template, which is subsequently amplified by the primer immobilized on microspheres. Hybridization of the detection probes to the elongated product results in high fluorescence signals that can be detected in a flow cytometer. If a padlock probe with a mutated locus anneals with a wild-type target, no circular template can be formed, and therefore no amplified signal can be detected.

Reaction conditions were chosen carefully to ensure successful detection of SNPs using this microsphere-based assay. The padlock probe and target were hybridized at 45 °C to reduce the secondary structures and enhance the hybridization efficiency, because secondary structures were found on the padlock probes termini with melting temperatures around 48 °C and would impede the binding of the probes to the targets (Supporting Information Figure S1). Reaction durations were also optimized to attain high assay sensitivity. We found out that the RCA products got entangled with each other easily if the RCA time went beyond 30 min, which triggered bead aggregation. Sonication or vigorous vortexing could break up the beads, but it also sheared the long product strand, hampering the quantification accuracy and precision. Assay reproducibility was impacted drastically as well due to the random breakage of the long DNA strands. Therefore, we kept the RCA duration at 30 min.

Padlock probe concentration and bead numbers play important roles on assay sensitivity as well. It seemed that binding of the padlock probe to both the target and the capture probe was not very efficient. We observed significant fluorescence signal enhancement with the same target concentraction only when the average number of padlock probe molecules per bead was tens or even hundreds times more than that of the capture probe on each bead. Higher circular probe concentration compared to that of the target and capture probe is needed to facilitate binding and improve detection sensitivity. Hence, 50 nM of the padlock probe was used in the following studies. On the other hand, since the primers are immobilized on the microspheres, using more beads in the assay can help to capture more circular templates for amplification. Nevertheless, beads compete with each other for the circular templates, and using more beads may lower the signal intensity on each bead. As the bead numbers increased from 3×10^4 to 5×10^5 with constant target and padlock probe concentrations at 20 and 40 nM, respectively, the fluorescent signal first increased, then dropped significantly once the bead numbers were over 1×10^5 (Supporting Information Figure S3). Therefore, 1×10^5 beads were employed in the following studies.

Sensitive and Specific Detection of Individual SNPs. Next, we tested the performance of this microsphere-based assay in SNPs detection. The padlock probe of Kras-G12C-M, oligonucleotide of Target-Kras-M, and CP1-coupled beads were used to mimic detection of G12C mutation in the K-ras gene. Fifty nanomolar padlock probe was mixed with 0−50 nM target in 40 μL of reaction buffer, and the circularized template was amplified on microspheres. The median fluorescence intensity was plotted against the target concentration in Figure 2a which showed a dynamic range extending more than 4 orders of magnitude. Even though the readings from 0.01 and 0.1 pM were relatively higher than that of the blank, significant signal increase was observed between 0.1 and 0.5 pM. Using the average standard deviation (SD) within the target concentration range of 0−0.5 pM, we calculated the theoretical 3 SD limit of detection to be 0.25 pM (10 attomol molecules). The SD and relative SD (RSD) at 0.5 pM were extremely high in this particular experiment, reaching 20 fluorescence units (SD) and 27% (RSD), whereas the RSD at other target concentrations was 16% to 2% across the entire analytical range with an average value of 11%. Several factors can contribute to the variations in fluorescence measurements. For instance, conglomeration of the large RCA products can prevent efficient binding of the detection probes which would impact the fluorescence signal. Entanglement and shearing of the long RCA products can happen during incubation on the tube rotator, affecting the final detection signals. Therefore, controlling the experimental conditions precisely is very critical to ensure high assay reproducibility. The same reasons can be used to explain the decreased fluorescence signal at 50 nM. At this concentration severe bead aggregation occurred, and stringent vortexing condition was needed to break up the beads, which might shear the long RCA product and decrease the fluorescence signal. Larger reaction volume or smaller bead numbers can be employed to alleviate this problem.

(39) Luo, J.; Bergstrom, D. E.; Barany, F. *Nucleic Acids Res.* **1996**, *24*, 3071−3078.

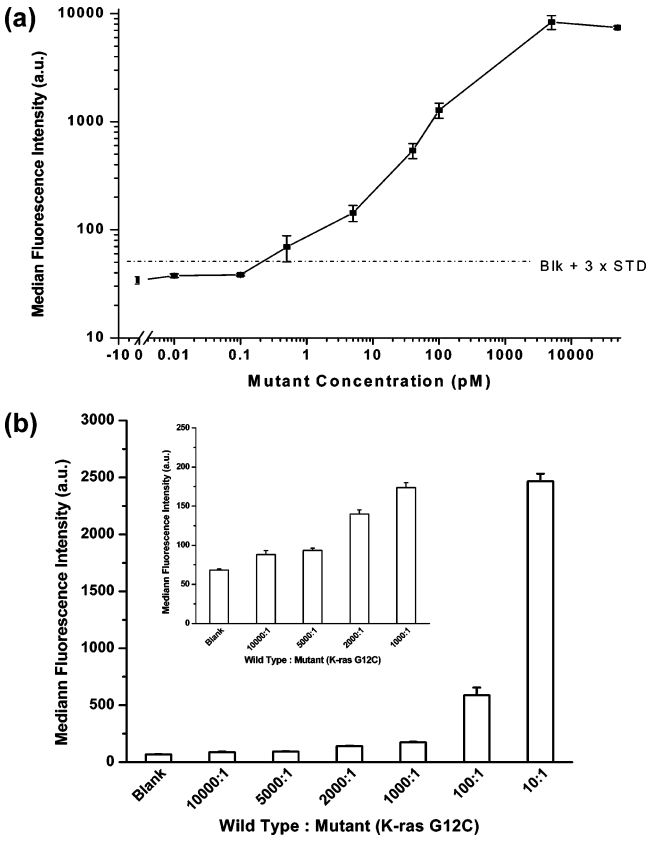

Figure 2. (a) Titration curve of the microsphere-based assay for detection of single-point mutation. The dotted line represents the fluorescence level 3 times the average standard deviation (SD) above the blank. (b) Effect of wild-type to mutant ratio to detection of mutant.

Still, the high sensitivity and large dynamic range make our microsphere-based assay unique, which can be attributed to the high polymerization efficiency of the DNA polymerase Phi29, the excellent detection sensitivity of the flow cytometer, and the dimension of the microsphere. Phi29 can add nucleotides to the amplification primer at a rate of 2280 nt/min and produce single-stranded DNA products more than 10^5 nucleotides long within 30 min.[33,40,41] Therefore, hundreds of the detection probes could attach to each of the long products in our case, resulting in an extremely high fluorescent signal. Added upon the efficient signal amplification are the high detection sensitivity with the flow cytometer and its fast flow rate that permits counting of thousands of particles in a few minutes and consequently improves the statistic reliability of the data. The feasibility in microsphere handling facilitates thorough washing, and the large surface area-to-volume ratio of microspheres offers high binding capacity, further enhancing the assay sensitivity.

To evaluate an SNP detection assay, sensitivity and specificity are the two most important measurements because they reflect the assay's ability of not sending out false negative or false positive signals.[7] Excellent performances in both aspects are necessities to adapt the assay to clinical applications. The specificity of our microsphere-based RCA assay is in general determined by the fidelity of the DNA ligase. Among the common commercially available DNA ligases, *Tth* and *E. Coli* ligase have been proved to be more sensitive to mismatched bases than T4 ligase.[39,42,43] However, the operating temperature of *Tth* (65 °C) is much higher than the melting temperatures of our padlock probes (around 58 °C). Instead, *E. Coli* ligase has an operating temperature of 37 °C and was employed in our study. Choosing experimental conditions carefully may help to improve the accuracy in SNP determination as well, because the elevated hybridization temperature may decrease the stability of the mismatched heteroduplexes. To assess the specificity of our assay, we mixed the oligonucleotides of Target-Kras-N and Target-Kras-M at different mole ratios of 10 000:1, 5000:1, 2000:1, 1000:1, 100:1, and 10:1 with a total concentration of 50 nM. These two strands represent the wild-type (N) and mutant (M) targets of K-ras G12C. The blank reaction contained 50 nM of the wild-type target only. The padlock probe of Kras-G12C-M with complementary sequence to the mutant target was added to the reaction at 50 nM. The results are displayed in Figure 2b. We can see from it that the median fluorescence intensity increased substantially from an average reading of 68.3 to 88.0 with a margin equal to 6 times SD when only 5 pM Target-Kras-M was added to the blank mixture (a wild-type strands to mutant ratio of 10 000:1). This result well demonstrates the extraordinary capability of our microsphere-based RCA assay in detecting a scarce mutation among a large quantity of wild types, which, along with the high sensitivity and wide dynamic range, grants the assay great potential in clinical applications of disease early diagnosis and prognosis.

Typing of Multiple SNPs with Dual-Color Detection and Two Bead Populations. Even within one codon, several SNPs could exist. Two or more alternative bases could occur on one locus, or different loci could exist on the same codon.[1] It is estimated that over 300 000 common SNPs will be required to map most of the variations in the genome, presenting a daunting challenge over any SNP screening assay on its accuracy, sensitivity, cost, and throughput.[1,3,13,27] Like planar arrays, microsphere-based suspension array can be performed in a high-throughput manner if beads with distinct optical or size properties are used as the discrete array elements.[35,36] For instance, the xMAP technology utilizes 100 types of particles with identical sizes but different doping levels of the internal fluorescent dyes which can be distinguished in a special flow cytometer, the Luminex instrument.[44] Regular flow cytometers can also be used to carry out medium throughput analysis if particles with different sizes are employed. Additionally, the modern flow cytometers, like the FACSAria, have advanced optical systems to perform multicolor analysis. The array throughput can then be further improved by using detection probes tagged with different fluorescent dyes.

Therefore, it is possible to achieve multiplexed detection of SNPs with our microsphere-based RCA assay if multiple fluoro-

(40) Soengas, M. S.; Gutierrez, M. S.; Salas, M. *J. Mol. Biol.* **1995**, *253*, 517−529.
(41) Lizardi, P. M.; Huang, X.; Zhu, Z.; Bray-Ward, P.; Thomas, D. C.; Ward, D. C. *Nat. Genet.* **1998**, *19*, 225−232.
(42) Tong, J.; Cao, W.; Barany, F. *Nucleic Acids Res.* **1999**, *27*, 788−794.
(43) Liu, L.; Tang, Z.; Wang, K.; Tan, W.; Li, J.; Guo, Q.; Meng, X.; Ma, C. *Analyst* **2005**, *130*, 350−357.
(44) Kettman, J. R.; Davies, T.; Chandler, D.; Oliver, K. G.; Fulton, R. J. *Cytometry* **1998**, *33*, 234−243.

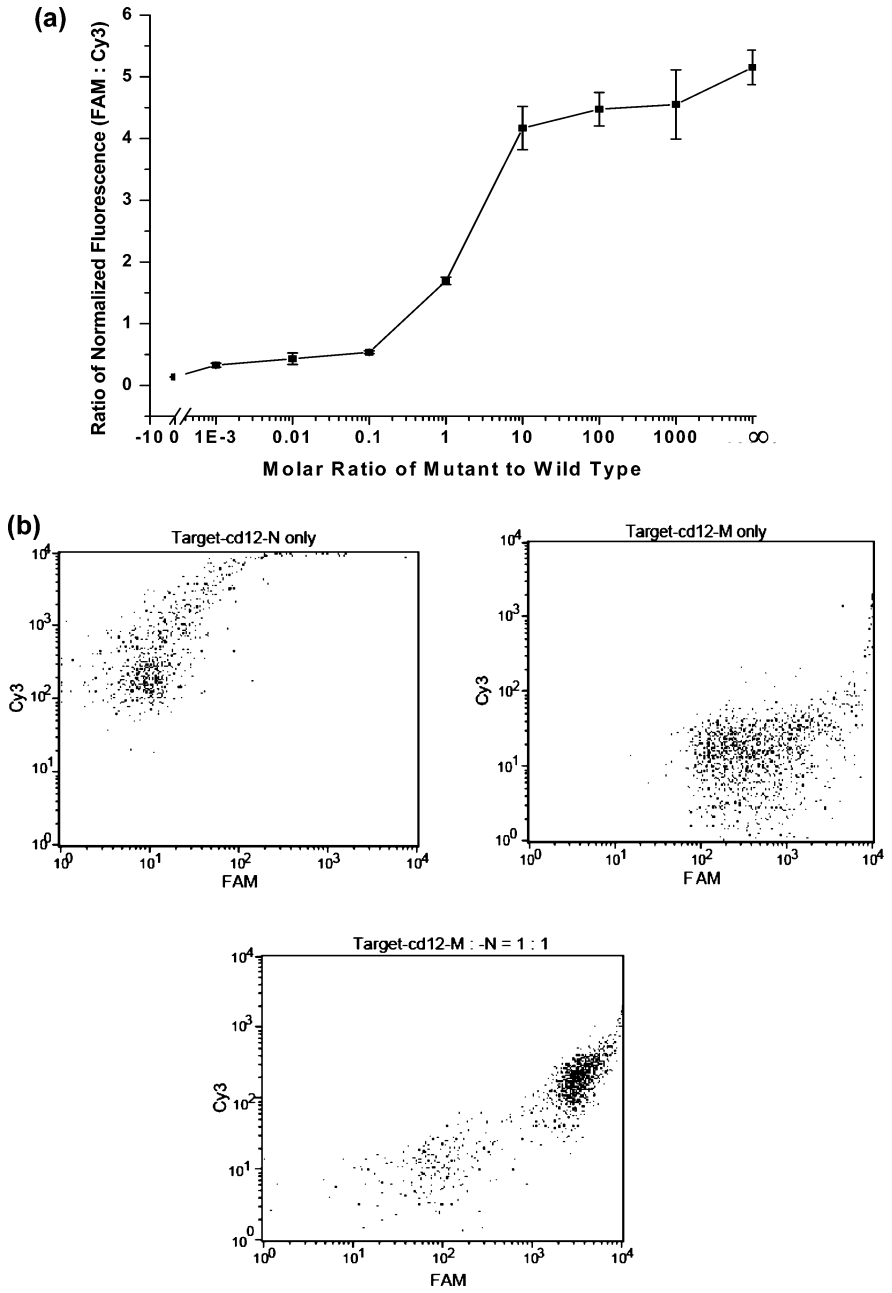

Figure 3. (a) Relationship between the ratio of adjusted fluorescence intensities from FAM and Cy3 and the ratio of mutant to wild type. (b) Dot plots for dual-color detections of both the wild-type and mutant targets in the flow cytometer.

phores and different bead populations are employed. We first tested this probability by using dual fluorescence tags to probe for sample heterozygosity. To our knowledge, this was the first attempt to use dual detection probes on one type of beads. Two padlock probes with one base difference at the end of the 3′ arm in the target binding region ("T" on Kras-G12C-M, and "G" on Kras-G12C-N) were employed to recognize the K-ras G12C mutation (GGT → TGT). It has been shown that DNA ligase exhibits greater discrimination against all single-base mismatches on the 3′ side of the nick in comparison with those on the 5′ side.[39,42,43] Both padlock probes can be captured by the CP1-coupled beads but bind to different detection probes. FAM-labeled DP1 anneals with the RCA products from Kras-G12C-M (mutant), and Cy3-labeled DP2 anneals with those from Kras-G12C-N (wild-types). FAM and Cy3 are both small fluorochromes that would not induce too much space hindrance in labeling the highly compact RCA products. Even though the excitation spectrum of FAM has some overlap with that of the Cy3 in the region of 560−570 nm, this dye combination was effective in our proof-of-principal study with compensation adjustments.

We mixed Target-Kras-N and Target-Kras-M at different molar ratios with a total target concentration of 1 nM, and the reactions contained 50 nM of both the padlock probes. Since the absolute fluorescence intensities from FAM and Cy3 are not comparable due to their different quantum yields and nonequivalent detector responses, we normalized the fluorescence from FAM and Cy3 against their own backgrounds and plotted the calibration curve (Figure 3a) using the normalized fluorescence ratio (FAM to Cy3) and the target molar ratio (mutant to wild-type). The relative

intensity of FAM to Cy3 gradually increased with the target molar ratios, which were 0, 0.001, 0.01, 0.1, 1, 10, 100, and 1000. The ratio of "∞" represented the result with 1 nM of the mutant target only, which showed much higher signal intensity ratio than the 1000:1 mixture. Again, the SDs were relatively high due to the bead aggregation at high mutant concentrations. Further investigations on reaction conditions are necessary for better control of the assay reproducibility in order to obtain more accurate measurements. Three representative dot plots of Fl1 versus Fl2 from reactions with pure wild-type target, equimolar mixture of the wild-type and mutant targets, and pure mutant target, correspondingly, are shown in Figure 3b. High fluorescence readings were found in the Fl2 (Cy3) channel with low detector response in the Fl1 (FAM) channel when only the Target-Kras-N was in the reaction, which is shown in the plot with dots occupying the upper-left panel only. Similarly, with only the Target-Kras-M, fluorescence signals dominate the lower-right panel on the dot plot. Strong signals in both the Cy3 and FAM channels were detected for the equimolar target mixture. There was still noticeable cross talk between the two detector channels when the fluorescence intensity was higher than 10^3. Collecting the median fluorescence instead of the arithmetic or geometric means could reduce the impact from cross talk, because the median, the value above and below which 50% of the distribution can be found, is less susceptible to the influence of outliers than the other two values.[45] By using nanocrystals with less spectrum overlaps, or flow cytometers with more detection channels, better detection performance can be achieved.

With this novel dual-color detection scheme, the typing throughput of our assay is improved by 2 times so that we can not only detect the positive existence of either sequence but obtain information about their relative quantities as well. By changing the last one or two bases on the 3′ arm, we can evaluate the sample heterozygosity or examine the presence of multiple mutations on the same codon. Incorporation of more fluorophores into the assay is also possible with the advanced flow cytometers that have more detection channels. For example, FACSAria has nine detection channels and theoretically can be employed to monitor nine different types of mutations on the same microsphere.

Moreover, utilization of microspheres with different properties can further enhance the assay throughput. Each padlock probe carries an allele-specific sequence for target recognition, a "zip-code" sequence for hybridization to specific microspheres, and a binding site for the detection probes. Varying the zip-code sequence, we can design padlock probes that bind to microspheres with different sizes or other properties. Designing padlock probes for high-throughput SNPs screening using this microsphere-based assay will not be more complex than constructing oligonucleotides for a universal DNA microarray or other SNP genotyping assays, such as the GoldenGate assays.[1,23,46] It is actually simpler because no PCR is involved that requires matching melting temperatures for all the probes, and the RCA rate has no dependence on template sequences.

Mutations of K-ras G12C and TP53 R372H were used in our demonstration of SNPs typing with the microsphere-based RCA assay. Two beads populations, each with a distinct size, were used to capture the padlock probes designated to K-ras G12C or TP53 R273H detection. The padlock probes for K-ras bound to the CP1-coupled beads (5.28 μm), which showed up in the R2 region on the light-scattering plot in Figure 4, and those for TP53 were captured by the CP2-coupled beads (3.17 μm) that occupied the R1 region. The Cy3 fluorescence still represented signals from the wild-type samples, and the FAM fluorescence was for the mutants. Therefore, in the fluorescence dot plots shown in Figure 4, reaction with equimolar mixture of the four target strands (Target-Kras-M/N, and Target-TP53-M/N) at a concentration of 5 nM resulted in equivalent Cy3 and FAM fluorescence in both the R1 and R2 regions.

SNPs Typing in PCR Amplicons Generated from Human Genomic DNA. The capability of our assay to detect SNPs in different genes can be used to check the co-occurrence of point mutations, which may represent a synergistic evolutionary pathway of tumor development or may influence mechanisms of chromosomal instability.[1,46] Point mutations in the proto-oncogene K-ras and the tumor suppressor TP53 are among the most common genetic alterations associated with the development and progression of human cancer. The mutational status and the specific mutation in these two genes have been shown to impact both tumor prognosis and response to therapies. Human genomic DNA extracted from human cell lines of HT29 and NCI-H358 were used in our study. According to the Catalog of Somatic Mutations in Cancer (http://www.sanger.ac.uk/genetics/CGP/cosmic/), HT29 contains a wild-type K-ras G12C and a mutated TP53 R273H. NCI-H358 has the K-ras G12C mutation but a total deletion of the TP53 gene. Because the assay reaction conditions were optimized using short oligonucleotides, direct ligation and RCA with genomic DNA was not performed in our study. Instead, PCR amplicons were used. However, with some modifications to the reaction conditions, such as genomic DNA digestion with restriction enzymes, the assay could be applied to genomic DNA without PCR amplification considering its high detection sensitivity demonstrated in our study.

PCR amplicons were generated from the genomic DNA of NCI-H238 and HT29. Amplicons from NCI-H358 was used with the CP1-coupled beads for the detection of K-ras G12C mutation, and those from HT29 were tested with the CP1- and CP2-coupled beads for parallel detection of the K-ras G12C and TP53 R273H mutations. Because a real blank with wild-type sequences of both SNPs was not available to us during the study, the control PCR product from λ DNA in the PCR kit was used as the negative control. As we mentioned before, direct comparison of the fluorescence signals from FAM and Cy3 was not meaningful due to the differences in detector responses and quantum yields; the signals were normalized against the corresponding blanks (Supporting Information Table 1S). The ratios of adjusted fluorescence from FAM and Cy3 were calculated and are listed in Table 2. The mutant to wild-type ratio in the samples was also estimated using the adjusted fluorescence ratio and the titration curve in Figure 3a and is listed in Table 2. This estimation was not entirely appropriate because the titration was done with synthetic oligonucleotide targets instead of PCR products. However, the change of sample types should impact the reaction efficiency to the same extend regardless of the target sequence or product labeling.

(45) Shapiro, H. M. *Practical Flow Cytometry*, 4th ed.; Wiley-Liss: New Jersey, 2002.
(46) Schneider, G.; Schmid, R. M. *Mol. Cancer* [Online] **2003**, 2:15. http://www.molecular-cancer.com/content/2/1/15.

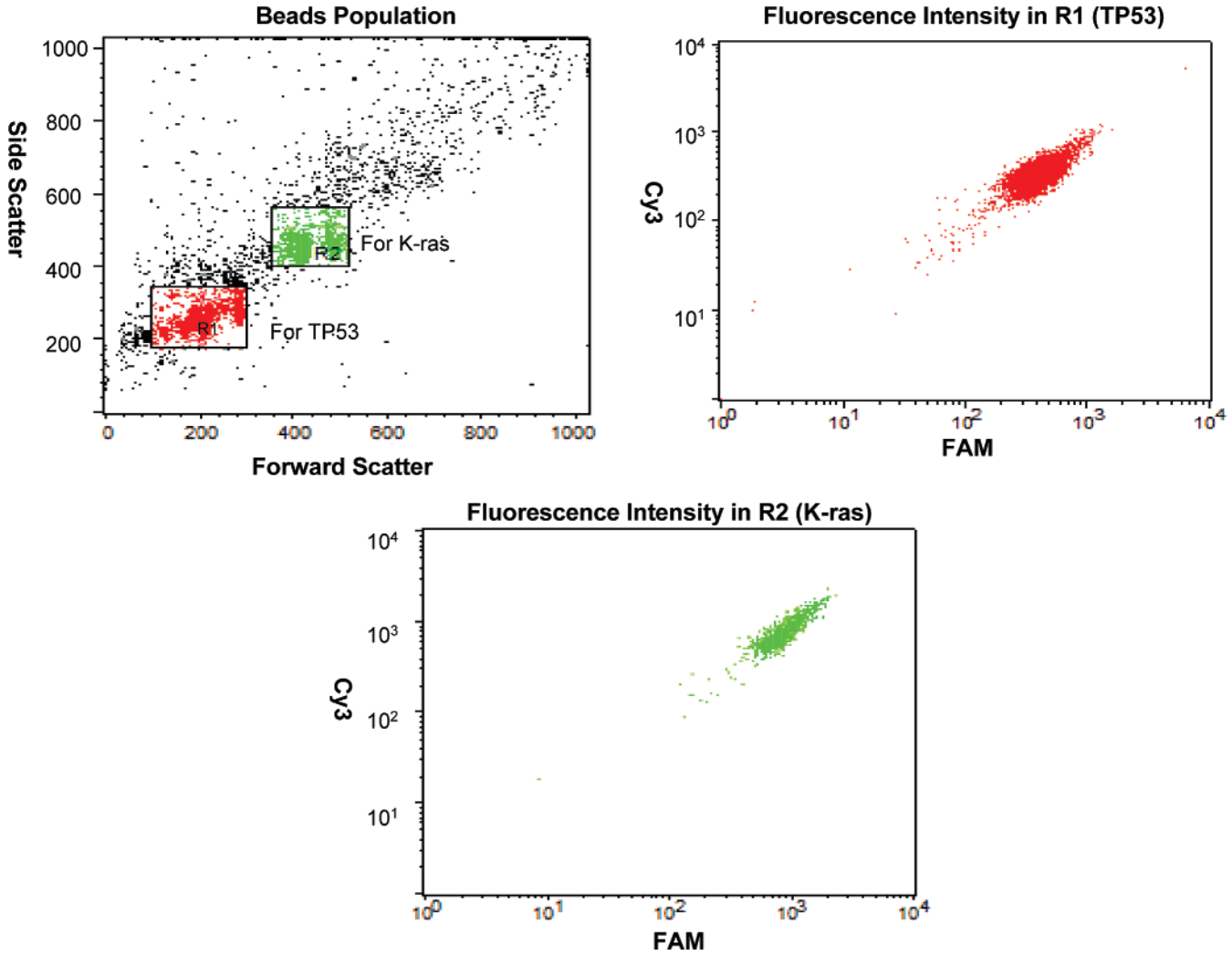

Figure 4. Flow cytometric dot plots for simultaneous detection of the wild-type and mutated sequences on different genes using the dual-color detection scheme and microspheres with different sizes.

Table 2. Typing of SNPs in PCR Products Generated from Genomic DNAs Extracted from the Cell Lines of HT29 and NCI-H358

cell line	SNP	ratio of normalized fluorescence	estimated mutant to wild-type ratio
H358	K-ras G12C	1.6	0.8
HT29	K-ras G12C	0.3	9.0×10^{-4}
	TP53 R273H	4.5	1.2×10^{3}

Therefore, it should not affect the relationship between relative signal ratio and target molar ratio too much, and our estimation should be sufficient for the proof-of-principle study. Our results showed that the genomic DNA from NCI-H358 contained both the mutant and the wild-type sequences of G12C at a ratio of 1.6. On the contrary, HT29 had a relatively pure wild type of K-ras G12C with a mutant to wild-type ratio less than 1×10^{-3} and a pure mutant of TP53 R273H with a mutant to wild-type ratio over 1000. Because our characterization of the heterozygosity of the sample from NCI-H358 was contradicted with information found in the literature, DNA sequencing was carried out on the PCRproducts only to verify our typing results, where both the mutant and the wild type of K-ras G12C were detected in the sample from NCI-H358 at a similar ratio and only one situation, either wild type (for TP53 R273H) or mutant (for K-ras G12C), was detected in the sample from HT29. The accuracy of the microsphere-based RCA assay in SNP determination was confirmed using this gold standard. Experiments with PCR products from genomic DNAs were only simple demonstrations of the multiplexing capability of our assay. Future investigations to directly apply our assay on unamplified genomic DNA samples and to test the confidence level of the assay in SNP typing with a large number of genomic samples are needed.

CONCLUSIONS

A highly sensitive and specific microsphere-based assay was developed to detect SNPs. The assay depends on the high fidelity of DNA ligase to generate a circular template upon recognition of a single-point mutation. The template is then amplified by the Phi29 polymerase, which has strand displacement ability, on the surface of microspheres. The elongation product remains attached to the microspheres and thus can be detected in a flow cytometer, indicating the mutation occurrence. A detection limit down to the low-picomolar level was achieved with the relatively simple assay design mainly because of the high amplification efficiency of Phi29 and the high binding capacity on the three-dimensional micro-

sphere surface. In addition, the remarkable precision of DNA ligase in distinguishing the mismatched bases at the ligation site led to the detection of low-abundant mutant with the coexistence of 10 000 times more wild-type targets. With further optimization of the reaction conditions, the assay should be able to perform direct SNPs detection from genomic DNAs.

Moreover, a novel dual-color detection scheme was employed to enhance the assay throughput by detecting both the wild-type and mutant strands with only one type of bead. Typing of different mutation alleles on two genes was demonstrated in our study with PCR amplicons generated from genomic DNA extracts. The assay throughput can be further improved if the xMAP technology with 100 types of microspheres is employed or multiple fluorophores and multiple beads sizes are used in an advanced flow cytometer with more detection channels available. The fast reaction kinetics and high binding capacity with the suspension array technology, combined with the high fidelity of the ligation, nondiscrimination over strand sequences of the RCA, and the isothermal reaction conditions, render to this microsphere-based RCA assay unique properties compared to the existing assays, such as simplicity in reaction schemes, extraordinary specificity and sensitivity, reduced complexity in assay design, easy handling, etc.

ACKNOWLEDGMENT

The authors thank Dr. Yinsheng Wang for using the Thermocycler in his group, and Barbara Walter of the Genomics Institute Core Instrument Facility for her assistance with the FACScan. This work was supported by U.C. Riverside.

SUPPORTING INFORMATION AVAILABLE

Additional information as noted in text. This material is available free of charge via the Internet at http://pubs.acs.org.

Received for review August 10, 2007. Accepted September 17, 2007.

AC701702T